

# Electromyograph and Keystroke Dynamics for Spoof-Resistant Biometric Authentication

Shreyas Venugopalan\*, Felix Juefei-Xu\*, Benjamin Cowley, and Marios Savvides  
CyLab Biometrics Center, Electrical and Computer Engineering  
Carnegie Mellon University, Pittsburgh, PA 15213, USA

{svenugop, juefeix, bcowley}@andrew.cmu.edu, msavvid@ri.cmu.edu

## Abstract

Biometrics has come a long way over the past decade in terms of technologies and devices that are used to verify user identities. Three of the more well studied modalities in this field are the face, iris and fingerprint, with the latter two reporting very high user identification/verification rates. In the biometric community there has been little work in studying biomedical signals for user recognition purposes. In this paper, we propose using electromyograph (EMG) signals as a person's biometric signature. The EMG records the motor unit action potentials (MUAP) during any physical motion. Our study is done within the context of a person using a keyboard to type a password or any other fixed phrase. Along with EMG signals, we log key press times for the user and study the feasibility of using this data too as a biometric feature. Keypress timings alone if used as a biometric, are very easy to spoof and hence we fuse this modality with EMG signals. In order to classify these features, we use subspace modeling as well as Bayesian classifiers. The experiments have been performed within the context of a user typing a fixed pass phrase at a workstation. The idea is to monitor both biometric modalities when this action is performed and study user verification across data capture sessions and within capture sessions. Our approach yields high values of verification rates, which shows the promise of using these modalities as user specific biometric signatures.

## 1. Introduction

The field of biomedical signal processing has taken great strides in the past two decades due to significant advances in biomedical measuring devices and instrumentation. Biomedical modalities such as Magnetic Resonance Imaging (MRI) and Positron Emission Tomography (PET)

\*These authors contribute equally to this work, and should be considered co-first authors.

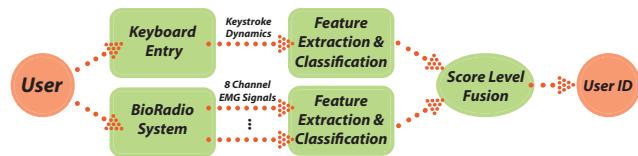


Figure 1. Our proposed experimental setup. We gather both EMG as well as keystroke dynamic data as the user types a fixed phrase on a keyboard. Various features are extracted from this data as detailed in later sections. We report user identification/verification scores when using either modality as a biometric.

enable physicians to visualize organ structures in three dimensions and perform diagnoses based on these images. Electroencephalography (EEG) signals monitor brain activity and have provided insights into human cognition and into neuro-science in general. There has also been a lot of work in the field of human computer interaction, using these signals. Another signal of interest is the electrocardiogram (ECG), which measures the electrical activity of the heart over a period of time. These signals have been used successfully to diagnose irregularities in the functioning of the heart. The use of biomedical signals for user identification however is a relatively less explored area. ECG alone has been explored as a biometric modality [30, 37]. Besides these, there has been little work in the use of biomedical signals for biometric based identify verification.

This article details our initial study on the use of the electromyograph (EMG) as a biometric, along with keystroke timing dynamics. The former refers to electric impulses measured from motor neurons, that initiate muscle activity, while the latter refers to timing information when striking the keys of a keyboard. Both of these are recorded as a user types on a keyboard. We also explore the possibility of fusion of information from both modalities. The data captured from every user is limited to a fixed text phrase typed on a keyboard (we operate under the assumption that the subject has to type in a password before accessing information from a workstation - both keystroke timings and EMG

signals are recorded as he/she types in this password). An outline of our experimental setup is shown in Figure 1. Typically, a muscle is composed of several motor units (MUs). Any EMG measurement performed using surface electrodes on the skin, as done in our work, picks up the Motor Unit Action Potentials (MUAPs). These signals are currently used non-medically for gesture recognition [10] [33] and general signal classification [2]. They are also used in a wide range of medical fields of study, including neuromuscular diseases, kinesiology, and motor control disorders. In the next section, we list some of the past literature on the use of EMG as well as keystroke dynamics for various purposes, following which in section 3 we describe our data acquisition setup as well as the database used in our study. Section 4 describes the various features that were extracted from the EMG measurements as well as from the keystroke timing measurements. In section 5 we present results for user identification/verification experiments using both these feature sets. Finally, in section 6 we provide a summary and a few concluding remarks including directions for future work.

## 2. Previous Work

As mentioned earlier, the EMG signal is an electrical representation of neuromuscular activation during the contraction/relaxation of muscles. The EMG signals can be categorized into surface EMG and intramuscle EMG [25]. The surface myoelectric signal shows effectiveness in controlling powered upper limb prostheses. Most commercially available systems utilize the surface EMG signal. More recently, studies on using an implantable myoelectric sensor which measures the internal (intramuscular) EMG have been published. Hargrove *et al.* in [8] have shown comparisons of surface and intramuscular EMG signal based classification. EMG signal processing and classification techniques have gone through tremendous improvements since the early 1980s. Saridis and Gootee [34] published one of the earliest works on EMG pattern analysis and classification for a prosthetic arm. Their algorithm was able to decompose the composite motion to the 6 primitive motions *i.e.* humeral rotation - in and out, elbow flexion and extension, and wrist pronation and supination. Other early works on EMG-aided arm prosthesis can be found in [5, 4]. More recently, Martelloni *et al.* [28] proposed that different objects can be identified using the EMG signal recorded from proximal arm muscles and they showed that the activation of proximal muscles can be statistically different for different grip types. Huang *et al.* [9] introduced the use of Gaussian Mixture Models (GMMs) for multiple limb motion classification using continuous myoelectric signals and show exceptional classification accuracy compared to linear discriminant analysis, linear perceptron network and multi-layer perceptron neural network.

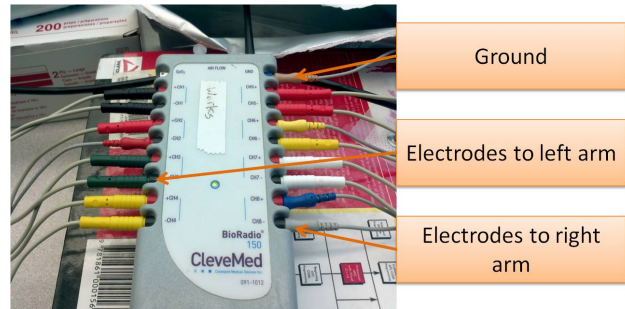


Figure 2. The Cleveland Medical Devices BioRadio used for measuring EMG signals in our experiments.

Along with EMG signals, the keystroke dynamics of users are also recorded during our data acquisition session (see section 3). By keystroke dynamics we refer to any feature related to the keys that a user presses such as key-down times, keyup times etc. In this work, we concentrate on classifying EMG and keystroke features for a fixed text, such as log on passwords, that is typed by a user. Gunetti and Picardi [7] have the best published results for text-free keystroke dynamics identification where they combine relative and absolute timing information on bigram, trigram and n-gram features. The classifier they adopted is related to k-nearest neighbors which does not scale well. Messerman *et al.* [29] dealt with the scalability issue but at the cost of accuracy. Although the authors' algorithm set an upper bound on the algorithm complexity, their proposed method is still computationally expensive. Killourhy *et al.* [26] tested static keystroke dynamic authentication on a dataset of 51 subjects, where each subject repeatedly typed a 10-character password 400 times. The authors reviewed and compared fourteen classification techniques on keystroke dynamics. The work by Zach *et al.* [42] used data limited to a 15ms resolution. Since some relevant features have an average duration shorter than this, the lack of timing precision can hide some discriminating information. Data collection with higher resolution is able to achieve a resolution of less than 0.1ms (see [38] for more details). There has been an increased interest in using additional information along with keystroke dynamics such as the keystroke sound [32] and user typing behavior [31].

Our aim, in this paper is to analyze both the EMG measurements as well as the keystroke dynamics of users and determine features that may be used to differentiate one individual from another. An advantage of using EMG signal alone is that, it is next to impossible to spoof one's EMG signal recording, unlike other modalities such as face (see [1, 18, 13, 12]) and iris (see [39]). Keystroke dynamics if used alone, can be spoofed by using information recorded in USB/PS2 keyboard buffers. A simple, timed replay of the keystrokes can be used to gain unauthorized access. In high security facilities where camera installations are not permit-

ted, this problem assumes a higher significance. Recording EMG signals along with the keystroke timings, allows us to perform a *liveness* test on the person entering the password, in addition to gaining a different biometric modality.

### 3. Acquisition of EMG Data

In this section, we present a description of how our data was acquired, as well as of the database built, for use in our experiments.

#### 3.1. Data Acquisition Sessions

The data was collected from a total of 14 participants. The acquisition process for a participant consisted of two *sessions*, which we will henceforth refer to as session I and session II. Each session consists of individual *trials*. During a trial, the participant types in the phrase “Hello, world.#18” followed by the ‘return’ key on a standard QWERTY keyboard. For every key press, using a custom built keylogger, we recorded the key pressed as well as the CPU time instant for key press and release. In addition, every time the participant types in the phrase, electrodes attached to his/her arm record the EMG signal using a BioRadio (see section 3.2 for a description). In this manner, during session I, 50 such trials were recorded. Session II was recorded more than 30 minutes after session I and includes 100 such trials from the same 14 participants. The keystroke features extracted include the keydown-to-keydown time, keyup-to-keydown time, and key hold time for each key in the typed phrase. For each trial, features were extracted and concatenated into a feature vector

#### 3.2. Recording EMG Activity Using BioRadio

The BioRadio device, shown in Figure 2, manufactured by Cleveland Medical Devices, Inc. was used to record the EMG signal during each participant’s trial as mentioned. BioRadio includes: (1) a wireless radio with USB interface to record the signal. (2) 17 snap MVAP II electrodes with 17 insulated snap leads. A pair of electrodes measures one channel of EMG data. 8 such channels (4 channels from each arm) were recorded by placing the electrodes on various portions of the arm. An additional electrode was used to ground the BioRadio. (3) a digital 5Hz high pass filter with 60 Hz notch filters on each channel. The filters are implemented on the BioLite software package available with the BioRadio device. Electrodes were placed on the skin above the hypothenar eminence, the thenar eminence, the extensor carpi ulnaris and anconeus, and the flexor carpi radialis and palmaris longus. Figure 3 shows the electrode placements for a participant. Using these, the surface voltages were recorded in mV at 960 Hz with a maximum voltage of 3V by the BioRadio.

The electrode pair recording the activity of the thenar eminence was intended to record much of the EMG data



Figure 3. The electrodes from BioRadio attached to both arms of a participant measure the EMG signal as he/she types the given phrase during a trial

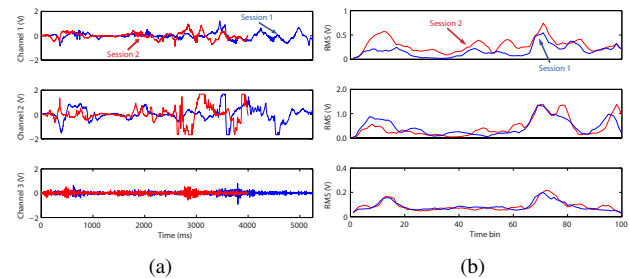


Figure 4. (a) Raw EMG data, showing three channels (out of a total of eight channels). The blue signal is a trial from Session 1, and red is a trial from Session 2. The Session 2 trial was recorded at least 30 minutes after Session 1. (b) The same EMG signals in (a) were partitioned into 100 time bins. The root-mean-square (RMS) was computed over each bin.

from the first finger (the forefinger), while the pair recording the hypothenar eminence was intended to record primarily from the small finger. The other two pairs were placed approximately on the anterior and posterior portions of the forearm. The electrode pair recording the carpi ulnaris and anconeus was intended to record data from the third finger (the “ring” finger). The pair recording the flexor carpi radialis and palmaris longus was intended to record the second (the “middle” finger). We placed electrodes over these regions after a visual inspection of which muscles were most prominent near the skin while the subject makes typing motions. In Figure 4 we show three channels of EMG recording for the same user from two different sessions.

#### 3.3. Keystroke Dynamics Measurements

As mentioned earlier, using a custom key logger routine, we recorded the key up and key down instant CPU times for every trial. The character length of the phrase typed, including the ‘return’ is 18. From the recorded timing, we computed keydown-to-keydown times (time lapse between key presses of consecutive keys), keyup-to-keydown times (time lapse between the release of one key and the press of the next key), and the hold times (time lapse between the press and release of each key) for all keys. This is illustrated in Figure 5. Hence, for each typing,  $18 \times 3 + 1 = 55$

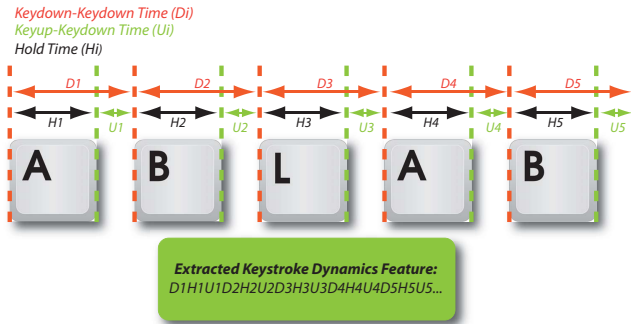


Figure 5. Example of keystroke dynamics features.

timing features were extracted and concatenated into a feature vector. These features are used independent of EMG data to identify participants in our experiments.

#### 4. Methods for EMG/Keystroke Classification

In this section we outline the various features extracted from the EMG signals for user identification. As mentioned in 3, all the data was collected in two sessions, with the person typing a fixed phrase on a keyboard. Each EMG trial within a session is segmented out using the timing information recorded by the keylogger. The experiments described in this paper were meant to: (1) study the variation in the EMG signal for a given subject, in a given session and extract features from all trials within a session, for the purpose of user identification. Higher identification rates in these experiments will make these features useful in continuous authentication scenarios. Since there are two recording sessions, two sets of equivalent experiments will be performed in each case. Any experiment using samples from session I alone will henceforth be termed  $E_1$  and those involving samples solely from session II will be termed  $E_2$ . (2) study the user identification rates when samples are compared across capture sessions. In this set of experiments, we have used data (either all or a subset) from session I as training samples. User identification was then performed on samples drawn from session II. These experiments will be termed as  $E_3$ .

In most of our experiments, we have used all trials from session I (which has fewer trials per user) as the training data for our supervised learning classifiers and trials from session II as the testing data. One of the intrinsic problems we faced during our experiments was that, trials for a subject are not of equal length (since the user does not type the same sequence in the same amount of time each trial). One way to overcome this issue is to crop every trial to the shortest trial's length. However, this method is not favorable, as it assumes the user has finished most of the keystrokes within that time. Our solution was to divide the trial into  $M$  non-overlapping bins. We then compute the root-mean-

square (RMS) value for each bin. Hence, for eight channels, we are left with an  $8M$  feature for each trial. This method has multiple advantages: (1) every trial (within a class and across classes) has the same number of time bins, and (2) trials are better aligned. Additionally, the RMS value also serves a denoising purpose. In the following sections, every trial has been represented in this manner. Figure 4 shows three channels from the EMG of a user, from two different sessions, overlaid on each other. As is evident from the figure, binning the data helps in smoothing out the variation and make the data from different sessions look more similar to each other.

#### 4.1. Using the Raw EMG Signal

Our first experiment, used the data samples such as those shown in Figure 4(b), as features. A distance matrix, which we call a *similarity matrix* with *one-to-one* Euclidean distance between every pair of samples was generated. Following this, each sample A was classified as belonging to the class represented by the sample B to which it is closest. More formally, if  $S$  is our similarity matrix,  $s_{i,j}$  represents the Euclidean distance between samples  $i$  and  $j$ . In order to classify for instance, the first sample, we find a sample  $l$  such that  $s_{l,1} = \min \{s_{j,1} | j = 1, 2, \dots, N\}$ . We classify the first sample as the class to which  $l$  belongs. Following this approach, the identification rates for the experiments  $E_1$ ,  $E_2$  and  $E_3$  are reported in Table 1.

#### 4.2. Bayesian Classifiers

As mentioned in section 3 we collected data from each user over the course of two sessions - 50 trials in session I and 100 trials in session II. In this section we estimate the Probability Density Function (PDF) corresponding to each user (we use the terms 'user' and 'class' interchangeably in the following text) using all the samples from session I. Given these PDFs, for every sample in session II, we can estimate a likelihood value and can then assign a class label to it based on the maximum likelihood estimate (MLE). We adopt two approaches to density estimation in this work - a non-parametric approach using the k-Nearest Neighbor (k-NN) method (see [6]) and a parametric approach where we fit a Gaussian distribution to the samples in session I.

##### Non-parametric Density Estimation Using k-NN

In our approach, rather than computing the density estimate for every point in the feature space, we associate a likelihood function with each data sample in session II, based on its  $k$  nearest neighbors from session I. Consider a 'test' data sample  $\mathbf{x}_i$ , from session II. Among its  $k$  nearest neighbors let  $\{k_1, k_2, \dots, k_N\}$  be the number of neighbors belonging to classes  $\lambda_1, \lambda_2, \dots, \lambda_N$  respectively. We define the likelihood of  $\mathbf{x}_i$  belonging to class  $\lambda_l$  as

$$P(\mathbf{x} = \mathbf{x}_i | \lambda = \lambda_l) = \frac{k_l}{k} \quad (1)$$

Now, consider the expression for Bayes rule,

$$P(\lambda = \lambda_l | \mathbf{x} = \mathbf{x}_i) = \frac{P(\mathbf{x} = \mathbf{x}_i | \lambda = \lambda_l) P(\lambda = \lambda_l)}{P(\mathbf{x} = \mathbf{x}_i)}$$

where  $P(\lambda | \mathbf{x})$  is the posterior probability (*i.e.* of the class given the observations),  $P(\mathbf{x} | \lambda)$  is the likelihood (*i.e.* of the observations given the class),  $P(\lambda)$  is the prior distribution of the class and  $P(\mathbf{x})$  is the evidence (*i.e.* the probability of the observations). In order to classify a given test sample  $\mathbf{x}_i$ , we will pick the class  $\lambda_l$  that maximizes  $P(\lambda = \lambda_l | \mathbf{x} = \mathbf{x}_i)$  based on our observations. In our experiments we assume a uniform prior over all classes and hence this problem degenerates to a maximum likelihood classifier *i.e.* we pick the class that maximizes  $P(\mathbf{x} = \mathbf{x}_i | \lambda = \lambda_l)$ . Hence, the class with the maximum likelihood (ML) to which  $\mathbf{x}$  belongs is given by

$$\begin{aligned} \hat{\lambda} &= \operatorname{argmin}_{l \in \{1, 2, \dots, N\}} P(\mathbf{x} = \mathbf{x}_i | \lambda = \lambda_l) \\ &= \operatorname{argmin}_{l \in \{1, 2, \dots, N\}} \frac{k_l}{k} \end{aligned} \quad (2)$$

#### Fitting a Gaussian Distribution

If we assume the  $d$  dimensional samples,  $\mathbf{x}$ , from every class has a Gaussian distribution (shown in eqn. (3)),

$$\mathcal{N}(\mathbf{x} | \mu, \Sigma) = \frac{1}{(2\pi|\Sigma|)^{d/2}} \exp\left(-\frac{(\mathbf{x} - \mu)^T \Sigma^{-1} (\mathbf{x} - \mu)}{2}\right) \quad (3)$$

then from the data in session I, we can estimate the density function parameters. Formally, for a given sample  $\mathbf{x}_i$ ,  $P(\mathbf{x} = \mathbf{x}_i | \lambda = \lambda_l) = \mathcal{N}(\mathbf{x} = \mathbf{x}_i | \mu_c, \Sigma_c)$  where  $\mathcal{N}(\mu, \Sigma)$  denotes a Gaussian distribution with mean  $\mu$  and covariance  $\Sigma$ . For each class  $\lambda_l$ , with  $K_l$  samples in session I, we can estimate the parameters as,

$$\mu_l = \frac{1}{K_l} \sum_{i=1}^{K_l} \mathbf{x}_i \quad (4)$$

$$\Sigma_l = \frac{1}{K_l} \sum_{i=1}^{K_l} (\mathbf{x}_i - \mu_l)(\mathbf{x}_i - \mu_l)^T \quad (5)$$

The ML estimate of the class label for a given data sample from session II is given by,

$$\hat{\lambda} = \operatorname{argmin}_{l \in \{1, 2, \dots, N\}} \mathcal{N}(\mathbf{x} = \mathbf{x}_i | \mu_l, \Sigma_l) \quad (6)$$

### 4.3. Linear Subspace Modeling

In addition, we have utilized the following three linear subspace learning methods: Principal Component Analysis (PCA), Unsupervised Discriminant Projection (UDP) [41, 16, 22, 20] and Class-Dependent Feature Analysis (CFA) [40, 19, 14, 15] for modeling the signals in various linear subspaces and perform matching tasks using the corresponding subspace features.

Using EMG			
	Raw Signal	PCA	SOS
$E_1$	98.67	96.33	82.83
$E_2$	96.94	96.43	81.28
$E_3$	40.00	-	32.26

Table 1. Rank 1 ID Rates when performing one-to-one comparisons between subject trials using recorded EMG data alone from 14 participants.

## 5. Experiments and Results

In this section we present the results obtained during our identification and verification experiments, using the features that were described in the previous section. We use data from two acquisition sessions, as mentioned in the previous section. We will refer to users as ‘classes’ in the following text (short for ‘user classes’). Session I contains 600 samples in total, of both EMG data and keystroke dynamics data, while session II contains 1175 samples from both modalities.

### 5.1. Using Trials from a Single Capture Session

A one-to-one comparison using the euclidean distance metric was performed. Rank 1 identification rates obtained are shown in Table 1. As described in section 4,  $E_1$  refers to one-to-one comparisons using only session I data,  $E_2$  refers to comparisons using only session II data.  $E_3$  refers to the experiment when samples in session II were compared with samples in session I and classified accordingly. For PCA experiment  $E_1$ , a subspace was built with samples in session II and session I samples were projected onto this space before one-to-one comparisons; vice versa for PCA experiment  $E_2$ . In this table, we also explore the possibility of using the Second Order Statistics (SOS) of the trials for classification purposes. Specifically, we use the power spectra of the signals as features for this purpose. Ideally, we would expect the power spectra of samples corresponding to a user within a single session to resemble each other. We see that this is indeed the case as shown by the results of the  $E_1$  and  $E_2$  experiments. However the identification rate drops when comparing power spectra across sessions.

From the identification rates obtained, it is evident that within a given session, the recorded signals are very similar to each other. The challenge is to identify users across sessions, which is discussed next. By just comparing the raw signals themselves, we get an identification rate of 40% as seen in Table 1. Next, we performed a set of verification experiments, in which we set a threshold for the similarity scores between samples and found the rate of false accepts and genuine accepts. The result is visualized using a set of Receiver Operating Characteristic (ROC) curves. In Figure 6(a) we show the ROC curves when classifying the EMG signals using various subspace modeling techniques presented in the previous section. We built subspace models

Using EMG Signals			
	GAR at 0.1% FAR	GAR at 1.0% FAR	GAR at 10% FAR
PCA	0.113	0.201	0.442
UDP	0.270	0.432	0.668
CFA	0.250	0.417	0.652
kNN	-	-	0.973

Table 2. GAR for various FAR in our user verification experiments that employ subspace modeling. The corresponding ROC curves are shown in Figure 6(a).

using the signals from session I and ran verification experiments using the signals from session II. The x-axis in these curves is shown in the log-scale to better depict the variation in Genuine Accept Rate (GAR) with varying False Accept Rates (FAR). Relevant values from these curves are given in Table 2.

## 5.2. Identifying Users from Trials Across Sessions

In order to classify individuals between sessions, as discussed in sections 4.2 and 4.2 we estimated the PDFs for each class using all the samples from session I. Following this, we classified samples from session II using ML estimates. The identification rate for the kNN based density estimation is 62.30%, while the identification rate when a Gaussian distribution is fit on the training samples is 48.68%, which are higher experiment  $E_3$  identification rates than those reported in Table 1. In this work we have used  $k = 10$ . The ROC curves for both these experiments are shown in Figure 6(b) (the x-axis is in the log-scale). As seen in Figure 6(b), we obtain above 90% verification rates for low values of false accept rate using both these methods. We see that the kNN based density estimation reports a better MLE based classification accuracy. Intuitively, the distribution of samples may not be strictly Gaussian and hence the Gaussian distribution based classifier may be too restrictive.

In addition the reader should note that the ROC curves are reported starting from a false accept rate (FAR) of 10% for the bayesian classifiers. This is because, these ROCs are generated by varying a probability threshold value and not distance metric values as in Figure 6(a) and Figure 6(c). Due to the limited number of users, 14, available to us for these set of experiments, the probability of assigning a class label to a given user cannot be less than  $\frac{1}{14} \approx 7\%$ . Hence, we cannot perform our verification experiments with threshold probability values lesser than this. With this minimum threshold, there are a large number of false accepts. However the genuine accepts are much higher as seen in the corresponding curves (even higher than the corresponding values in the subspace based classifiers; for example compare the GAR at 10% FAR for the ROCs in Figure 6(a) and in Figure 6(b)). All Bayesian classifier based results reported in this work are reported starting from an FAR of 10%.

Using Keystroke Dynamics			
	GAR at 0.1% FAR	GAR at 1% FAR	GAR at 10% FAR
PCA	0.213	0.382	0.658
UDP	0.364	0.491	0.683
CFA	0.348	0.444	0.667
kNN	-	-	0.994

Table 3. GAR at various FAR for keystroke dynamics recognition experiments using 3 subspace modeling techniques.

## 5.3. Identification Using Keystroke Features

We report our classification results that were obtained using the extracted keystroke features *i.e.* the keydown-keydown times, keyup-keydown time and the hold times (as was mentioned in section 3). Table 3 shows the GAR at 0.1%, 1% and 10% FAR, using the three subspace modeling techniques. Figure 6(c) shows the ROC curves of the corresponding experiments. As can be seen, UDP yields the best results for these features. All the experiments mentioned in the table are of type  $E_2$  where trials from session II were used for testing. The training samples required for PCA, CFA and UDP were drawn from session I.

## 5.4. Score Level Fusion

Here we report results on the verification performance when we performed score level fusion of results obtained using both modalities *i.e.* EMG and keystroke dynamics. The score level fusion was performed by taking the magnitude of a score vector whose individual elements were corresponding scores from the EMG based classifier and the keystroke dynamics based classifier, *i.e.*

$$\text{score}_{fused} = \sqrt{(\text{score}_{EMG})^2 + (\text{score}_{Keystroke})^2} \quad (7)$$

The general trend observed is an increase in verification performance as can be seen from the ROC curves. In Figure 6(d) we compare the result of the  $E_2$  set of experiments for both modalities, when using the raw input signals values. We see that there is a clear improvement as indicated by the improved genuine accept rates (see Table 4). A comparison of the performance when fusing raw EMG signals with various keystroke dynamics classification methods is shown in Figure 6(e). We see that the highest genuine acceptance rates are obtained when the score level fusion uses the UDP based classifier. Compared to other subspace modeling techniques such as linear discriminant analysis (LDA), UDP handles outliers better due to its unsupervised characteristics. In real-world application, instances of the same subject may not appear to be within a perfect cluster. This may due to mis-labeling or simply noise embedded in the system. Such noise will jeopardize supervised methods such as LDA which entirely rely on the class label/centroid information.

In Figure 6(f) we compare the performance of the best subspace based classifiers we have reported in this work so

Performance after Fusion of Scores			
	GAR at 0.1% FAR	GAR at 1% FAR	GAR at 10% FAR
Raw EMG + Raw KeyStroke	0.301	0.463	0.683
Raw EMG + PCA KeyStroke	0.306	0.503	0.701
Raw EMG + UDP KeyStroke	0.390	0.547	0.731
Raw EMG + CFA KeyStroke	0.343	0.510	0.702
UDP EMG + UDP KeyStroke	0.247	0.411	0.661
UDP EMG + CFA KeyStroke	0.321	0.424	0.619
CFA EMG + UDP KeyStroke	0.369	0.569	0.801
CFA EMG + CFA KeyStroke	0.334	0.546	0.788
kNN EMG + kNN KeyStroke	-	-	0.997
SVM EMG + SVM KeyStroke	-	-	0.987

Table 4. GAR at various FAR for the fusion of EMG and Keystroke.

far. We fused the scores from the UDP and CFA based classifiers for both the EMG and keystroke dynamics signals. The fusion of the CFA based EMG classifier and UDP based keystroke classifier is observed to have an edge over the rest in terms of verification performance. Relevant genuine acceptance rates are shown in Table 4.

In Figure 6(g) we compare the performance of the kNN based classifier, described earlier for the EMG features, on both the EMG as well as keystroke dynamics feature sets. In this case the keystroke dynamics based feature dominates and there is little improvement gained by fusing the results of the EMG feature set.

### 5.5. Support Vector Machines Experiments

In addition to the above set of experiments, we trained a linear Support Vector Machine (SVM) model for both EMG and keystroke dynamics data in UDP subspace. The training data consists of the 600 samples (collected in session I) and our testing data, as before, are the samples from session II. The SVM classifier fits a distribution to the sample distances from the linear hyperplane used by the SVM model, thus enabling us to compute the probability of class membership for a given test sample. Thus given an SVM for class  $\lambda_i$  and a feature  $\mathbf{x}_i$  we can estimate the maximum likelihood class label in the same manner as described in section 4.2. We used the libSVM library [3] in our experiments.

Summarizing this section, we note the following salient points based on the results reported: (1) Subspace modeling techniques show promise in verifying users when the individual scores from both EMG based and keystroke dynamics based classifiers are fused. We see genuine acceptance rates of close to 80% using CFA based EMG classification and UDP based keystroke dynamics classification. The use of an SVM model trained in UDP space results in an improvement in verification performance as shown in Table 4. (2) In order to achieve a better verification performance, we adopted Bayesian based approaches. Specifically, a kNN based probability density estimation was performed for the various classes present in session I. Following this, session II samples were classified using a maximum likelihood ap-

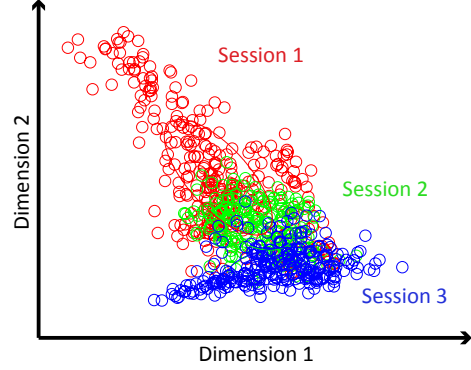


Figure 7. 2-dimensional projection of an 8-dimensional RMS space. Each circle represents one trial; colors denote different sessions from the same subject.

proach. Due to the limited number of samples and classes, we were not able to evaluate the effectiveness of this approach at very low values of FAR and hence report results from 10% FAR onwards. We see that these values are higher than the corresponding values for the subspace modeling based approaches.

## 6. Conclusions

In this paper, we have explored the possibility of using both electromyograph (EMG) signals from arm muscles as well as keystroke dynamics of a person as biometric modalities. The data was captured when a user typed a fixed phrase on a keyboard. As mentioned earlier, EMG signals are next to impossible to spoof unlike keystroke dynamics, which can be recorded and played back by an imposter using a simple USB/PS2 external buffer. Recording EMG signals along with keystroke timing dynamics, is a *liveness* test on the person entering the password, in addition to gaining a different biometric modality. In this work, keystrokes serve a dual purpose of segmenting different EMG trials as well. This paper reports the results from an initial study on the use of biometric features from both these modalities as well as from a fusion of these. subspace modeling techniques were used in our verification experiments. From Table 4, we see that a fusion of results from the CFA based EMG classifier and UDP based keystroke dynamics classifier gives high rates of genuine accepts at low values of false accepts. In order to improve identification and verification rates when comparing user data captured across two sessions, we build PDFs for the EMG data using both non-parameteric (based on kNN) and parameteric (based on Gaussian distribution) models. Corresponding genuine acceptance rates (GAR) are above 90% for very low values of false accept rates as shown in Figure 6(b).

Analyzing the acquired EMG data, we have found many areas for improvement in both feature selection and classi-

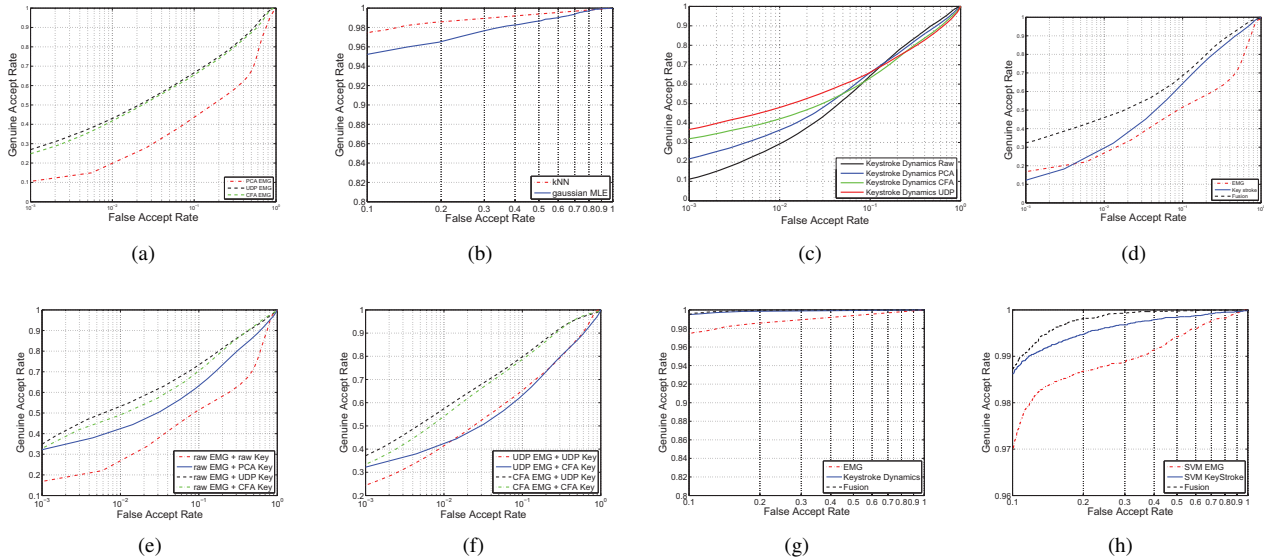


Figure 6. (a): ROC curves for EMG features based verification using various subspace modeling techniques. (b): The ROC curves for EMG using density model based Bayesian classifiers. We see that the kNN based MLE classifier reports higher verification rates when compared to the Gaussian model based MLE classifier. The latter may be too restrictive an assumption for the actual data distribution. (c): ROC curves for keystroke dynamics recognition using various subspace modeling techniques. (d): ROC curves for EMG signal based verification experiment, the keystroke dynamics based verification experiment and using fusion of the two sets of scores. The experiments are the  $E_2$  based experiments described earlier, using one-to-one comparison of the signals. (e): ROC curves comparing the verification performance after fusion of scores from the indicated classification experiments. (f): ROC curves comparing the performance when fusing scores from the UDP and CFA based classifier for both the EMG signals and keystroke dynamics. We observe that the best performance is obtained when using the CFA classifier with EMG and UDP classifier with keystroke dynamics. (g): ROC curves comparing the performance of the k-NN based classifier using the EMG signals, using the keystroke dynamics and when scores from these two classifiers are fused. We see that the keystroke dynamics dominates in this experiment. Fusion results in a slight improvement in performance. (h): ROC curves comparing the performance of the SVM based classifier in UDP subspace using both EMG signals and keystroke dynamics. The ROC plotted using a fusion of the scores from the two classifiers is also shown.

fication. EMG signals contain considerable noise between trials, ranging from the intensity of a keystroke hit to different postures between sessions. Feature selection may be improved by utilizing methods other than RMS and also leveraging time-dependencies with dynamic time warping [27]. To improve parametric density estimation based classification, one may view the distribution and correlations between channels. By taking the RMS of each trial, we treat each trial as an  $8 \times 1$  vector in a high-dimensional space. We can take a 2D projection of this space and intuit how the distribution changes between sessions (see Figure 7; three sessions of a user are shown). Between sessions, the mean does change significantly, questioning the use of Gaussian parameters to describe the activity. Future work will need to account for the factors that lead to these changes between sessions. For example, posture, fatigue, and motivation may all affect EMG activity. By correctly modeling such changes, both parametric and non-parametric density estimation based methods will improve greatly.

We feel that this preliminary work proves the presence of a biometric modality in these recordings. The aim of our

future work is two fold - to study the feasibility of using EMG/keystrokes for continuous user authentication during a typing session and to be able to recognize users across capture sessions. The results in this paper show that this is indeed possible, and we hope to study this modality further and develop it into a stronger biometric such as face, iris, and gait [17, 36, 35, 23, 24, 21, 11]. In addition, with the future development of wearable technologies such as smart wrist band, the continuous monitoring of the EMG signals along with the keystroke dynamics can be made possible for non-intrusive and spoof-robust biometric authentication.

## 7. Acknowledgement

We would like to thank Professor Tom Sullivan from the Department of Electrical and Computer Engineering at Carnegie Mellon University for his very helpful input during the course of this work. We would also like to thank our colleagues Aaron Jaech and Benjamin Shimamura for their help during our data capture sessions and for help in interpreting the data.

## References

- [1] A. Adler. Images can be regenerated from quantized biometric match score data. In *Electrical and Computer Engineering, 2004. Canadian Conference on*, volume 1, pages 469–472 Vol.1, may 2004. 2
- [2] M. Ahsan, M. Ibrahimy, and O. Khalifa. EMG signal classification for human computer interaction: A review. *European Journal of Scientific Research*, 33(3):480–501, 2009. 2
- [3] C.-C. Chang and C.-J. Lin. LIBSVM: A library for support vector machines. *ACM Transactions on Intelligent Systems and Technology*, 2:27:1–27:27, 2011. Software available at <http://www.csie.ntu.edu.tw/~cjlin/libsvm>. 7
- [4] D. C. Dening, F. G. Gray, and R. M. Haralick. Prosthesis control using a nearest neighbor electromyographic pattern classifier. *Biomedical Engineering, IEEE Transactions on*, BME-30(6):356–360, june 1983. 2
- [5] P. C. Doerschuk, D. E. Gustafon, and A. S. Willsky. Upper extremity limb function discrimination using emg signal analysis. *Biomedical Engineering, IEEE Transactions on*, BME-30(1):18–29, jan. 1983. 2
- [6] R. O. Duda, P. E. Hart, and D. G. Stork. *Pattern Classification (2nd Edition)*. Wiley-Interscience, 2 edition, Nov. 2001. 4
- [7] D. Gunetti and C. Picardi. Keystroke analysis of free text. *ACM Transactions on Information and System Security (TISSEC)*, 8(3):312–347, aug 2005. 2
- [8] L. Hargrove, K. Englehart, and B. Hudgins. A comparison of surface and intramuscular myoelectric signal classification. *Biomedical Engineering, IEEE Transactions on*, 54(5):847–853, may 2007. 2
- [9] Y. Huang, K. Englehart, B. Hudgins, and A. Chan. A gaussian mixture model based classification scheme for myoelectric control of powered upper limb prostheses. *Biomedical Engineering, IEEE Transactions on*, 52(11):1801–1811, nov. 2005. 2
- [10] P. Ju, L. P. Kaelbling, and Y. Singer. State-based classification of finger gestures from electromyographic signals. In *ICML*, pages 439–446, 2000. 2
- [11] F. Juefei-Xu, C. Bhagavatula, A. Jaech, U. Prasad, and M. Savvides. Gait-ID on the Move: Pace Independent Human Identification Using Cell Phone Accelerometer Dynamics. In *Biometrics: Theory, Applications and Systems (BTAS), 2012 IEEE Fifth International Conference on*, pages 8–15, Sept 2012. 8
- [12] F. Juefei-Xu, M. Cha, J. L. Heyman, S. Venugopalan, R. Abiantun, and M. Savvides. Robust Local Binary Pattern Feature Sets for Periocular Biometric Identification. In *Biometrics: Theory Applications and Systems (BTAS), 4th IEEE Int'l Conf. on*, pages 1–8, sep 2010. 2
- [13] F. Juefei-Xu, M. Cha, M. Savvides, S. Bedros, and J. Trojanova. Robust Periocular Biometric Recognition Using Multi-level Fusion of Various Local Feature Extraction Techniques. In *IEEE 17th International Conference on Digital Signal Processing (DSP)*, 2011. 2
- [14] F. Juefei-Xu, K. Luu, M. Savvides, T. Bui, and C. Suen. Investigating Age Invariant Face Recognition Based on Periocular Biometrics. In *Biometrics (IJCB), 2011 International Joint Conference on*, pages 1–7, Oct 2011. 5
- [15] F. Juefei-Xu, D. K. Pal, and M. Savvides. Hallucinating the Full Face from the Periocular Region via Dimensionally Weighted K-SVD. In *Computer Vision and Pattern Recognition Workshops (CVPRW), 2014 IEEE Conference on*, June 2014. 5
- [16] F. Juefei-Xu, D. K. Pal, and M. Savvides. NIR-VIS Heterogeneous Face Recognition via Cross-Spectral Joint Dictionary Learning and Reconstruction. In *Computer Vision and Pattern Recognition Workshops (CVPRW), 2015 IEEE Conference on*, June 2015. 5
- [17] F. Juefei-Xu, D. K. Pal, K. Singh, and M. Savvides. A Preliminary Investigation on the Sensitivity of COTS Face Recognition Systems to Forensic Analyst-style Face Processing for Occlusions. In *Computer Vision and Pattern Recognition Workshops (CVPRW), 2015 IEEE Conference on*, June 2015. 8
- [18] F. Juefei-Xu and M. Savvides. Can Your Eyebrows Tell Me Who You Are? In *Signal Processing and Communication Systems (ICSPCS), 2011 5th International Conference on*, pages 1–8, Dec 2011. 2
- [19] F. Juefei-Xu and M. Savvides. Unconstrained Periocular Biometric Acquisition and Recognition Using COTS PTZ Camera for Uncooperative and Non-cooperative Subjects. In *Applications of Computer Vision (WACV), 2012 IEEE Workshop on*, pages 201–208, Jan 2012. 5
- [20] F. Juefei-Xu and M. Savvides. An Augmented Linear Discriminant Analysis Approach for Identifying Identical Twins with the Aid of Facial Asymmetry Features. In *Computer Vision and Pattern Recognition Workshops (CVPRW), 2013 IEEE Conference on*, pages 56–63, June 2013. 5
- [21] F. Juefei-Xu and M. Savvides. An Image Statistics Approach towards Efficient and Robust Refinement for Landmarks on Facial Boundary. In *Biometrics: Theory, Applications and Systems (BTAS), 2013 IEEE Sixth International Conference on*, pages 1–8, Sept 2013. 8
- [22] F. Juefei-Xu and M. Savvides. Subspace Based Discrete Transform Encoded Local Binary Patterns Representations for Robust Periocular Matching on NIST's Face Recognition Grand Challenge. *IEEE Trans. on Image Processing*, 23(8):3490–3505, aug 2014. 5
- [23] F. Juefei-Xu and M. Savvides. Facial Ethnic Appearance Synthesis. In *Computer Vision - ECCV 2014 Workshops*, volume 8926 of *Lecture Notes in Computer Science*, pages 825–840. Springer International Publishing, 2015. 8
- [24] F. Juefei-Xu and M. Savvides. Weight-Optimal Local Binary Patterns. In *Computer Vision - ECCV 2014 Workshops*, volume 8926 of *Lecture Notes in Computer Science*, pages 148–159. Springer International Publishing, 2015. 8
- [25] E. Kamavuako, K. Englehart, W. Jensen, and D. Farina. Simultaneous and proportional force estimation in multiple degrees of freedom from intramuscular emg. *Biomedical Engineering, IEEE Transactions on*, 59(7):1804–1807, july 2012. 2
- [26] K. S. Killourhy and R. A. Maxion. Comparing anomaly-detection algorithms for keystroke dynamics. In *Proceed-*

- ings of the *IEEE International Conference on Dependable Systems and Networks (DSN)*, pages 125–134, jun 2009. 2
- [27] G. Li, Y. Wang, M. Li, and Z. Wu. Similarity match in time series streams under dynamic time warping distance. In *Computer Science and Software Engineering, 2008 International Conference on*, volume 4, pages 399–402, dec. 2008. 8
- [28] C. Martelloni, J. Carpaneto, and S. Micera. Characterization of emg patterns from proximal arm muscles during object- and orientation-specific grasps. *Biomedical Engineering, IEEE Transactions on*, 56(10):2529–2536, oct. 2009. 2
- [29] A. Messerman, T. Mustafic, S. A. Camtepe, and S. Albayrak. Continuous and non-intrusive identity verification in real-time environments based on free-text keystroke dynamics. In *Proceedings of the IEEE International Joint Conf. on Biometrics (IJCB)*, pages 1–8, oct 2011. 2
- [30] K. Plataniotis, D. Hatzinakos, and J. Lee. Ecg biometric recognition without fiducial detection. In *Biometric Consortium Conference, 2006 Biometrics Symposium: Special Session on Research at the*, pages 1–6, 19 2006-aug. 21 2006. 1
- [31] J. Roth, X. Liu, and D. Metaxas. On Continuous User Authentication via Typing Behavior. *IEEE Trans. on Image Processing*, 23(10):4611–4624, oct 2014. 2
- [32] J. Roth, X. Liu, A. Ross, and D. Metaxas. Investigating the Discriminative Power of Keystroke Sound. *IEEE Transactions on Information Forensics And Security (TIFS)*, 10(2):333–345, Feb 2015. 2
- [33] T. S. Saponas, D. S. Tan, D. Morris, J. Turner, and J. A. Landay. Making muscle-computer interfaces more practical. In *Proceedings of the 28th international conference on Human factors in computing systems, CHI '10*, pages 851–854, New York, NY, USA, 2010. ACM. 2
- [34] G. N. Saridis and T. P. Gootee. Emg pattern analysis and classification for a prosthetic arm. *Biomedical Engineering, IEEE Transactions on*, BME-29(6):403–412, june 1982. 2
- [35] M. Savvides and F. Juefei-Xu. Image Matching Using Subspace-Based Discrete Transform Encoded Local Binary Patterns, Sept. 2013. US Patent US 2014/0212044 A1. 8
- [36] K. Seshadri, F. Juefei-Xu, D. K. Pal, and M. Savvides. Driver Cell Phone Usage Detection on Strategic Highway Research Program (SHRP2) Face View Videos. In *Computer Vision and Pattern Recognition Workshops (CVPRW), 2015 IEEE Conference on*, June 2015. 8
- [37] T. Shen, W. Tompkins, and Y. Hu. One-lead ecg for identity verification. In *Engineering in Medicine and Biology, 2002. 24th Annual Conference and the Annual Fall Meeting of the Biomedical Engineering Society EMBS/BMES Conference, 2002. Proceedings of the Second Joint*, volume 1, pages 62–63 vol.1, 2002. 1
- [38] S. J. Shepherd. Continuous authentication by analysis of keyboard typing characteristics. In *European Convention on Security and Detection*, pages 111–114, may 1995. 2
- [39] S. Venugopalan and M. Savvides. How to generate spoofed irises from an iris code template. *Information Forensics and Security, IEEE Transactions on*, 6(2):385–395, June 2011. 2
- [40] B. V. K. Vijaya Kumar, M. Savvides, and C. Xie. Correlation pattern recognition for face recognition. *Proc. of the IEEE*, 94(11):1963–1976, nov 2006. 5
- [41] J. Yang, D. Zhang, J. Yang, and B. Niu. Globally maximizing, locally minimizing: Unsupervised discriminant projection with applications to face and palm biometrics. *IEEE Trans. Pattern Analysis and Machine Intelligence (TPAMI)*, 29:650–664, 2007. 5
- [42] R. S. Zack, C. C. Tappert, and S. H. Cha. Performance of a long-text-input keystroke biometric authentication system using an improved k-nearest-neighbor classification method. In *Proceedings of the Fourth IEEE International Conference on Biometrics: Theory Applications and Systems (BTAS)*, pages 1–6, sep 2010. 2